Molecular BioSystems

Accepted Manuscript

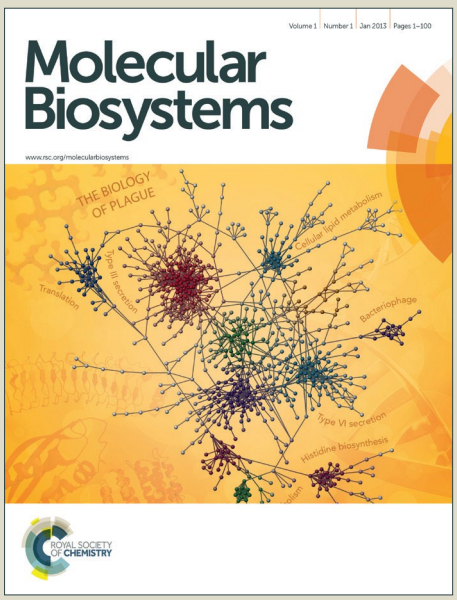

ROYAL SOCIETY OF CHEMISTRY

www.rsc.org/molecularbiosystems

Molecular Biosystems Molecular BioSystems Dynamic Article Links ▶

Cite this: DOI: 10.1039/c0xx00000x

www.rsc.org/xxxxxx

Communication

Oligomerization Enhancement and Two Domain Swapping Mode Detection for Thermostable Cytochrome c_{552} by Elongation of the Major Hinge Loop†

Chunguang Ren,[a] Satoshi Nagao,[a] Masaru Yamanaka,[a] Hirofumi Komori,[b] Yasuhito Shomura,[c,d] Yoshiki Higuchi,[c,d] and Shun Hirota*[a]

Received (in XXX, XXX) Xth XXXXXXXXX 20XX, Accepted Xth XXXXXXXXX 20XX
DOI: 10.1039/b000000x

High-order oligomers of *Hydrogenobacter thermophilus* cytochrome c_{552} increased as inserting more Gly residues between Ala18 and Lys19 at the major hinge loop of the wild-type protein. N-terminal and C-terminal domain swapping were elucidated by X-ray crystallography for the mutant with insertion of three Gly residues at the hinge loop.

Protein self-assemblies have been constructed by various groups utilizing well-established interactions, such as metal coordination,[1] chemical cross-linking,[2] host−guest interaction,[3] hydrophobic interaction,[4] and electrostatic interaction.[5] Structured protein oligomers may be used as building blocks to create diverse functional nanomaterials.[6] For example, well-ordered porphyrin clusters constructed with heme protein nanorings have been reported.[7] Proteins also self-assemble by three-dimensional (3D) domain swapping, which has been defined by Eisenberg and co-workers.[8] In domain swapping, a protein molecule exchanges its structural element or domain with the corresponding region of another molecule.[9] We have shown that heme proteins,[10] including horse cytochrome (cyt) *c*[10a] and *Hydrogenobacter thermophilus* (HT) cyt c_{552},[10b] domain swap. HT cyt c_{552} has three long α-helices, and His14 and Met59 are coordinated to the heme iron.[11] HT cyt c_{552} exhibits high stability, where the denaturation temperature of the oxidized protein is higher than 100 °C.[12] Different domain swapping modes (N-terminal and C-terminal regions) and different oligomerization orders have been observed for proteins in the same *c*-type cyt protein family. HT cyt c_{552} mainly forms small size oligomers by swapping the region containing the N-terminal α-helix and heme,[10b] whereas horse cyt *c* forms high-order oligomers larger than 50mers by swapping the C-terminal α-helix.[10a] Since the hinge loop of HT cyt c_{552} (Ala18Lys19Lys20) is shorter than that of horse cyt *c* (Thr78–Ala83), high-order oligomer formation may have been inhibited by the steric hindrance between the protomers in the HT cyt c_{552} oligomer.[10b] In this study, the amount of high-order oligomers increased by elongation of the hinge loop in HT cyt c_{552}. We also obtained two different thermostable domain-swapped dimers of the three Gly-inserted HT cyt c_{552} mutant, and elucidated their structures by X-ray crystallography, showing that domain swapping may occur at both N-terminal and C-terminal regions in HT cyt c_{552}.

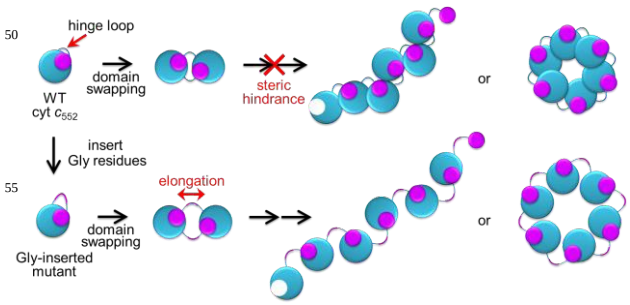

Fig. 1. Schematic view of insertion of Gly residues between Ala18 and Lys19 at the hinge loop of WT cyt c_{552} for formation of high-order oligomers.

We constructed HT cyt c_{552} mutants by inserting one (insG1), two (insG2) or three (insG3) Gly residues between Ala18 and Lys19 at the hinge loop of the wild-type (WT) protein to reduce the steric repulsion in the oligomers, so that the mutants may form high-order oligomers (Figure 1). Oxidized WT cyt c_{552} and its Gly-inserted mutants in 50 mM potassium phosphate buffer, pH 7.0, precipitated by an addition of ethanol (90% (v/v)). After the precipitate was lyophilized and dissolved in the same buffer, the amount of high-order oligomers (larger than decamers) eluting earlier than the elution volume of 13.7 mL in the size exclusion chromatogram obtained using Superdex 200 was ~1% against total protein for the WT protein (Figure 2a). The corresponding area for the mutants increased to ~5%, ~9% and ~10%, for insG1, insG2 and insG3, respectively, indicating formation of more high-order oligomers with increase in insertion of Gly residues at the hinge loop. These results show that the length and flexibility of the hinge loop affect the size

[a]*Graduate School of Mat*erials Scienc*e, Nara Institute of Science and Technology, 8916-5 Takayama, Ikoma, Nara 630-0192, Japan. E-mail: hirota@ms.naist.jp; Fax: (+81)-743-72-6119*
[b]*Faculty of Education, Kagawa University, 1-1 Saiwai, Takamatsu, Kagawa 760-8522, Japan.*
[c]*Department of Life Science, Graduate School of Life Science, University of Hyogo, 3-2-1 Koto, Kamigori-cho, Ako-gun, Hyogo 678-1297, Japan.*
[d]*RIKEN SPring-8 Center, 1-1-1 Koto, Sayo-cho, Sayo-gun, Hyogo 679-5148, Japan.*
†Electronic supplementary information (ESI) available: Full experimental details, crystallographic data, chromatograms and spectra. See DOI: 10.1039/ b000000x

and amount of domain-swapped oligomers. In addition, almost no oligomers dissociated by incubation at 50 °C for 1 h, indicating relatively high thermostability of the oligomers (Figure S1).

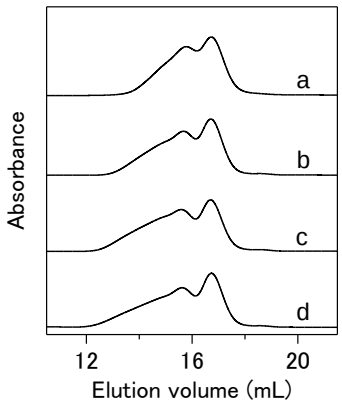

Fig. 2. Size exclusion chromatograms of WT and mutant cyt c_{552} after treatment with ethanol: (a) WT, (b) insG1 mutant, (c) insG2 mutant, and (d) insG3 mutant. After addition of ethanol up to 90% (v/v) to WT or mutant cyt c_{552} (500 μM) at 70 °C, the obtained precipitates were lyophilized, dissolved in buffer at 4 °C, and analysed with a Superdex 200 column.

The dimers exhibiting the peak with the second largest elution volume in the size exclusion chromatogram obtained using Superdex 75 (Figure S2) were further purified with cation exchange chromatography (Figure S3). Two peaks were observed in the cation exchange chromatograms of the WT and Gly-inserted mutant dimers, showing that two types of dimers existed for all the proteins investigated (Figure S3, curves a–d). However, the two dimers of the WT protein could not be separated by cation exchange chromatography, since the two dimer peaks were overlapped. The peaks of the two dimers separated more in the cation exchange chromatograms for the Gly-inserted mutants (Figure S3), and the two dimers (major and minor) were purified successfully for the insG3 mutant (Figure S3, curves c and d). The peak position of the insG3 major dimer in the cation exchange chromatogram was shifted from those of the insG3 minor dimer and WT dimers (Figure S3, curves e and f), presumably due to elongation of the hinge loop and change in the surface charge density of the insG3 major dimer compared to the WT dimers by the insertion of Gly residues. Since significant amount of high-order oligomers were obtained and the two dimers were purified for the insG3 mutant, we investigated the dimers and oligomers of the insG3 mutant in more detail.

Most of the major and minor insG3 dimers did not dissociate by incubation at 70 °C for 30 min (Figure S4), showing that the dimers were thermostable. However, the minor dimer dissociated by incubation at 80 °C for 30 min, whereas the major dimer did not dissociate by incubation at similar conditions (Figure S4). The maximum wavelength of the Soret band of oxidized insG3 major and minor dimers was 410 nm (Figure S5A), which was similar to that of the oxidized WT monomer. The absorption coefficient of the Soret band for both major and minor dimers was obtained as 109,000 ± 1000 M^{-1} cm^{-1} (heme unit) by the pyridine hemochrome method.[13] This value was also similar to the absorption coefficients obtained for the WT monomer (109,000 ± 2000 $M^{-1}cm^{-1}$) and insG3 monomer (109,000 ± 1000 $M^{-1}cm^{-1}$), and the reported value for the WT monomer (105,000 M^{-1} cm^{-1} at 409.5 nm).[14] In the circular dichroism spectra of oxidized insG3 major and minor dimers, negative Cotton effects were observed at 208 and 222 nm, where the intensities were similar to those of the WT and insG3 monomers (Figure S5B). These results indicated that the active site and secondary structures were similar among the monomers and dimers.

The structure of the insG3 major dimer at 1.26 Å resolution exhibited a domain-swapped structure, where the N-terminal region containing the heme (up to Lys17) was exchanged between protomers (PDB ID: 5AUR) (Figure 3B). The swapped region in the insG3 major dimer was similar to that reported for the WT dimer.[10b] The structure of the insG3 minor dimer at 1.30 Å resolution also exhibited a domain-swapped structure (PDB ID: 5AUS) (Figure 3C). Interestingly, the swapping region of the minor dimer was the C-terminal region (from Pro61), which was different from that of the WT and major dimers. Although multiple domain swapping modes have been reported for several non-heme proteins,[9, 15] the present result on cyt c_{552} is the first example for a heme protein to exhibit different modes of domain swapping, indicating that multiple mode domain swapping may also occur in heme proteins.

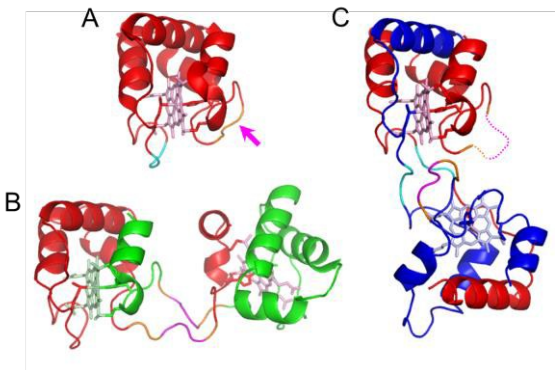

Fig. 3. Crystal structures of WT cyt c_{552} and its insG3 major and minor dimers: (A) WT monomer (PDB ID: 1YNR, red), (B) insG3 major dimer (PDB ID: 5AUR, red and green) and (C) insG3 minor dimer (PDB ID: 5AUS, red and blue). The hemes are shown as stick models in pale colours. Side-chain atoms of His14 and Met62 (Met59 for the WT monomer) are shown as stick models. The inserted residues (Gly19Gly20Gly21) are shown in pink. The pink arrow in the WT monomer structure represents the insertion position. The hinge loops of the major dimer are shown in orange and pink. The hinge loops of the minor dimer are shown in cyan. The dotted lines represent the residues with electron densities not detected.

The protein structures of the insG3 dimers corresponded well to that of the WT monomer (Figure S6). We calculated the root-mean-square deviation (rmsd) values for the Cα atoms between the structures of the insG3 major (minor) dimer and the WT monomer (four molecules in the asymmetric unit) (Table S1). Residues in the N-terminal region before the hinge loop of one protomer and residues in the C-terminal region after the hinge loop in the other protomer in the same insG3 major (minor) dimer were compared with the corresponding structural region of the monomer. The rmsd values of the major and minor

dimers were 0.25−0.35 Å and 0.32−0.45 Å, respectively. These results indicate that the structures were similar between the WT monomer and the protomers of the insG3 major and minor dimers. For the insG3 minor dimer, Gly19–Lys22 were undetectable in a protomer structure, due to their flexibility, and excluded for the calculations.

The heme iron coordination structure (Met−Fe−His) was similar among the WT monomer and both the insG3 major and minor dimers (Figure 4). Met62 coordinated to the heme in both insG3 dimers, but it originated from the other protomer to which the heme belonged. The Fe−His14 distance of the insG3 major and minor dimers was 2.04−2.07 Å and 2.04−2.05 Å, respectively, whereas the Fe−Met62 distance was 2.25−2.39 Å and 2.34−2.35 Å, respectively. These distances were similar to the corresponding distances in the WT monomer (Fe−His14, 2.05−2.09 Å; Fe−Met59, 2.33−2.40 Å) (Table S2). These results were consistent with the absorption spectra (Figure S5A), indicating that the active site structure was similar among the monomer and both dimers.

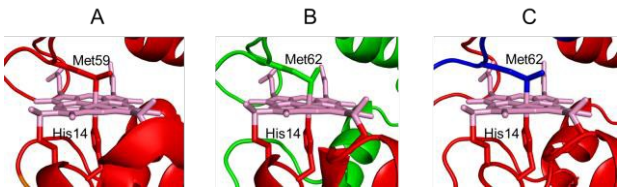

Fig. 4. Active site structures of WT cyt c_{552} and its insG3 major and minor dimers: (A) WT monomer (red), (B) insG3 major dimer (PDB ID: 5AUR) and (C) insG3 minor dimer (PDB ID: 5AUS). The hemes are shown in pink stick models. The red and green (or blue) strands in the insG3 major (or minor) dimer structure are regions from different protomers. Side-chain atoms of His14 and Met62 (Met59 for the monomer) are shown as stick models.

Negative staining transmission electron microscopy (TEM) was performed to investigate the morphology of insG3 oligomers from approximately the octamer to pentadecamer, purified by size exclusion chromatography. Unfortunately, we could not observe TEM images for isolated insG3 oligomers. We speculated that the hydrophobic property of the insG3 mutant inhibited the interaction of the protein with the staining compound, phosphotungstic acid, and thus replaced Trp57 of the insG3 mutant with Lys (insG3/W57K mutant). The insG3/W57K mutant formed high-order oligomers similar to the insG3 mutant by treatment with ethanol (Figure S7). The TEM image of oligomeric insG3/W57K mutant (from octamer to pentadecamer) exhibited well-separated protein ring structures at 7–10 nm in diameter (Figure 5). Although the size of the ring structures was at the resolution limit, observation of the ring images were reproducible (Figure S8). The region containing the N-terminal α-helix and heme is hydrophobic and forms a well-organized structure in cyt c_{552}, and thus this region would be unstable in aqua solution and may bind to the rest of the protein, resulting in formation of a ring-structured oligomer. Linear structures may also exist in the oligomers, but were undetectable, since the size of HT cyt c_{552} (~2 nm in diameter) was too small. Many double-ring structures were also observed in the TEM image. Major N-terminal and minor C-terminal domain swapping were observed in the insG3 dimer structures (Figure 3). By the C-terminal domain swapping, it is difficult to form high-order oligomers, since its hinge loop was constructed with only three residues, similar to the WT protein (Figure 2). Therefore, Gly-inserted cyt c_{552} molecules may domain swap the N-terminal region successively and form a ring structure, whereas the ring structures may be connected by domain swapping the C-terminal region. Construction of a protein nanoring has been reported by introducing specific interactions, such as metal ion chelation and chemical cross-linking.[1d, 2a] We constructed protein oligomers with a thermostable protein using domain swapping. Especially, the protein structure, including the active site, of the monomer is maintained in the oligomers produced by domain swapping. These results indicate that relatively strong interactions are necessary to obtain stable protein nanostructures, and domain swapping may be useful to control interaction between protein molecules and construct functional protein oligomers.

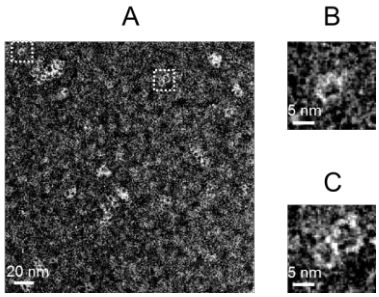

Fig. 5. Negative staining TEM image of insG3/W57K cyt c_{552} oligomers: (A) Overall view, expanded views of (B) single- and (C) double-ring structures.

In summary, we have succeeded in increasing the amount of high-order domain-swapped oligomers of thermostable HT cyt c_{552} by inserting Gly residues into the hinge loop. Major and minor insG3 dimers exhibited different domain-swapped structures, where the N-terminal region was exchanged between protomers for the major dimer and the C-terminal region for the minor dimer. Single- and double-ring structures were observed for the oligomers. These results show that domain swapping can be applied to construct protein nanostructures, providing a new design strategy for the construction of protein assemblies.

The authors thank Ms. Sakiko Fujita and Mr. Masahiro Fujihara, Nara Institute of Science and Technology (NAIST), for their technical assistance on TEM observation, and Mr. Leigh McDowell, NAIST, for his advice on manuscript preparation. The synchrotron radiation experiments were performed at the BL38B1 and BL44XU beamlines of SPring-8 with the approval of JASRI (No. 2014B1438 (S.N.) and No. 2015A6999 (H.K.)). The authors are grateful to Prof. Yoshihiro Sambongi, Hiroshima University, for a kind gift of pKO2 and pEC86 plasmid DNAs. This work was partially supported by Grants-in-Aid for Scientific Research (Category B, No. 26288080; S.H.) and Challenging Exploratory Research (No. 15K13744; S.H.) from JSPS.

Notes and references

1. (a) I. Medalsy, O. Dgany, M. Sowwan, H. Cohen, A. Yukashevska, S. G. Wolf, A. Wolf, A. Koster, O. Almog, I. Marton, Y. Pouny, A. Altman, O. Shoseyov and D. Porath, *Nano Lett.*, 2008, **8**, 473–477; (b) A. D. Malay, J. G. Heddle, S. Tomita, K. Iwasaki, N. Miyazaki, K. Sumitomo, H. Yanagi, I. Yamashita and Y. Uraoka, *Nano Lett.*, 2012, **12**, 2056–2059; (c) W. Zhang, Q. Luo, L. Miao, C. Hou, Y. Bai, Z. Dong, J. Xu and J. Liu, *Nanoscale*, 2012, **4**, 5847–5851; (d) Y. Bai, Q. Luo, W. Zhang, L. Miao, J. Xu, H. Li and J. Liu, *J. Am. Chem. Soc.*, 2013, **135**, 10966–10969.
2. (a) J. C. T. Carlson, S. S. Jena, M. Flenniken, T.-f. Chou, R. A. Siegel and C. R. Wagner, *J. Am. Chem. Soc.*, 2006, **128**, 7630–7638; (b) H. Kitagishi, K. Oohora, H. Yamaguchi, H. Sato, T. Matsuo, A. Harada and T. Hayashi, *J. Am. Chem. Soc.*, 2007, **129**, 10326–10327; (c) K. Oohora, S. Burazerovic, A. Onoda, Y. M. Wilson, T. R. Ward and T. Hayashi, *Angew. Chem. Int. Ed.*, 2012, **51**, 3818–3821.
3. C. Hou, J. Li, L. Zhao, W. Zhang, Q. Luo, Z. Dong, J. Xu and J. Liu, *Angew. Chem., Int. Ed.*, 2013, **52**, 5590–5593.
4. (a) M. J. Boerakker, J. M. Hannink, P. H. H. Bomans, P. M. Frederik, R. J. M. Nolte, E. M. Meijer and N. A. J. M. Sommerdijk, *Angew. Chem. Int. Ed.*, 2002, **41**, 4239–4241; (b) M. J. Boerakker, N. E. Botterhuis, P. H. H. Bomans, P. M. Frederik, E. M. Meijer, R. J. M. Nolte and N. A. J. M. Sommerdijk, *Chem. Eur. J.*, 2006, **12**, 6071–6080.
5. D. P. Patterson, M. Su, T. M. Franzmann, A. Sciore, G. Skiniotis and E. N. G. Marsh, *Protein Sci.*, 2014, **23**, 190–199.
6. (a) Y.-T. Lai, K.-L. Tsai, M. R. Sawaya, F. J. Asturias and T. O. Yeates, *J. Am. Chem. Soc.*, 2013, **135**, 7738–7743; (b) L. Miao, J. Han, H. Zhang, L. Zhao, C. Si, X. Zhang, C. Hou, Q. Luo, J. Xu and J. Liu, *ACS Nano*, 2014, **8**, 3743–3751; (c) S. Sim, D. Miyajima, T. Niwa, H. Taguchi and T. Aida, *J. Am. Chem. Soc.*, 2015, **137**, 4658–4661.
7. J.-H. Jeoung, D. A. Pippig, B. M. Martins, N. Wagener and H. Dobbek, *J. Mol. Biol.*, 2007, **368**, 1122–1131.
8. M. J. Bennett, S. Choe and D. Eisenberg, *Proc. Natl. Acad. Sci. U.S.A.*, 1994, **91**, 3127–3131.
9. (a) Y. Liu, P. J. Hart, M. P. Schlunegger and D. Eisenberg, *Proc. Natl. Acad. Sci. U.S.A.*, 1998, **95**, 3437–3442; (b) Y. Liu, G. Gotte, M. Libonati and D. Eisenberg, *Nat. Struct. Mol. Biol.*, 2001, **8**, 211–214.
10. (a) S. Hirota, Y. Hattori, S. Nagao, M. Taketa, H. Komori, H. Kamikubo, Z. Wang, I. Takahashi, S. Negi, Y. Sugiura, M. Kataoka and Y. Higuchi, *Proc. Natl. Acad. Sci. U.S.A.*, 2010, **107**, 12854–12859; (b) Y. Hayashi, S. Nagao, H. Osuka, H. Komori, Y. Higuchi and S. Hirota, *Biochemistry*, 2012, **51**, 8608–8616; (c) S. Nagao, H. Osuka, T. Yamada, T. Uni, Y. Shomura, K. Imai, Y. Higuchi and S. Hirota, *Dalton Trans.*, 2012, **41**, 11378–11385; (d) Y.-W. Lin, S. Nagao, M. Zhang, Y. Shomura, Y. Higuchi and S. Hirota, *Angew. Chem. Int. Ed.*, 2015, **54**, 511–515; (e) S. Nagao, M. Ueda, H. Osuka, H. Komori, H. Kamikubo, M. Kataoka, Y. Higuchi and S. Hirota, *PLoS ONE*, 2015, **10**, e0123653; (f) M. Yamanaka, S. Nagao, H. Komori, Y. Higuchi and S. Hirota, *Protein Sci.*, 2015, **24**, 366–375.
11. C. Travaglini-Allocatelli, S. Gianni, V. K. Dubey, A. Borgia, A. Di Matteo, D. Bonivento, F. Cutruzzolà, K. L. Bren and M. Brunori, *J. Biol. Chem.*, 2005, **280**, 25729–25734.
12. Y. Yamamoto, N. Terui, N. Tachiiri, K. Minakawa, H. Matsuo, T. Kameda, J. Hasegawa, Y. Sambongi, S. Uchiyama, Y. Kobayashi and Y. Igarashi, *J. Am. Chem. Soc.*, 2002, **124**, 11574–11575.
13. E. A. Berry and B. L. Trumpower, *Anal. Biochem.*, 1987, **161**, 1–15.
14. X. Wen and K. L. Bren, *Biochemistry*, 2005, **44**, 5225–5233.
15. (a) Y. Liu, G. Gotte, M. Libonati and D. Eisenberg, *Protein Sci.*, 2002, **11**, 371–380; (b) I.-J. L. Byeon, J. M. Louis and A. M. Gronenborn, *J. Mol. Biol.*, 2003, **333**, 141–152; (c) M. A. Schumacher, M. Crum and M. C. Miller, *Structure*, 2004, **12**, 849–860; (d) K.-E. Chen, A. A. Richards, J. K. Ariffin, I. L. Ross, M. J. Sweet, S. Kellie, B. Kobe and J. L. Martin, *Acta Crystallogr. D*, 2012, **68**, 637–648.